JOURNAL OF THE BULGARIAN GEOGRAPHICAL SOCIETY

Journal of the Bulgarian Geographical Society 51: 151–175 (2024)
DOI: 10.3897/jbgs.e136806

Research Article

Reducing uncertainty in future projections of potential evapotranspiration using a regional climate model and observational datasets: A case study of Egypt

Samy A. Anwar[1], Latifa Zhouri[2], Bilel Zerouali[3,4], Yong Jie Wong[5]

1 *Egyptian Meteorological Authority, Qobry EL-Kobba, Cairo, Egypt*
2 *Laboratory of Sustainable Agriculture Management, Higher School of Technology Sidi Bennour, Chouaib Doukkali University, El Jadida, Morocco*
3 *Laboratory of Architecture, Cities and Environment, Faculty of Civil Engineering and Architecture, Department of Hydraulic, Hassiba Benbouali, University of Chlef, B.P. 78C, Ouled Fares, Chlef 02180, Algeria*
4 *Vegetal Chemistry-Water-Energy Research Laboratory, Faculty of Civil Engineering and Architecture, Department of Hydraulic, Hassiba Benbouali, University of Chlef, B.P. 78C, Ouled Fares, Chlef 02180, Algeria*
5 *Department of Bioenvironmental Design, Faculty of Bioenvironmental Sciences, Kyoto University of Advanced Science, Kameoka 606-8501, Japan*

Corresponding author: Bilel Zerouali (b.zerouali@univ-chlef.dz)

Abstract

This study aims to reduce uncertainty in future projections of potential evapotranspiration (PET) across Egypt by utilizing the regional climate model (RegCM4) under two distinct Representative Concentration Pathways (RCP): RCP4.5 and RCP8.5. The RegCM4 was downscaled using the medium-resolution Earth System Model from the Max Planck Institute, achieving a horizontal resolution of 20 km over Egypt. Initially, the spatial distribution of simulated PET was assessed, followed by the correction of historical PET calculations using long-term gridded data from the Climate Research Unit (CRU) through a linear regression model (LRM) at twelve locations representing diverse climate zones in Egypt. The LRM was then applied to adjust future PET projections covering the period from 2006 to 2100. Significant spatial anomalies in PET were observed, particularly during the periods 2061–2080 and 2081–2100, with more pronounced anomalies under the RCP8.5 scenario compared to RCP4.5. Across all locations, the RegCM4 effectively captured the monthly variability of PET in relation to CRU data. Furthermore, the application of the LRM substantially improved the accuracy of simulated PET, demonstrating the effectiveness of this approach in enhancing model performance and reducing uncertainty in future projections.

Key words: Climate change, evapotranspiration uncertainty, Climate Research Unit, RegCM4, enhancing model, RCP scenarios, future projections

Academic editor: Stoyan Nedkov
Received: 10 September 2024
Accepted: 18 November 2024
Published: 06 December 2024

Citation: Anwar SA, Zhouri L, Zerouali B, Wong YJ (2024) Reducing uncertainty in future projections of potential evapotranspiration using a regional climate model and observational datasets: A case study of Egypt. Journal of the Bulgarian Geographical Society 51: 151–175. https://doi.org/10.3897/jbgs.e136806

1. Introduction

Water resource management stands as a pivotal challenge on the global stage, affecting numerous regions grappling with issues surrounding water availability and sustainability (Abda et al. 2022; Elbeltagi et al. 2023; Zerouali et al. 2024a). Nowhere is this concern more pronounced than in arid and semi-arid locales such as Egypt, where the spectre of water scarcity looms

large (Lasheen 2022; Anwar et al. 2023). In these environments, the accurate assessment and effective management of water resources emerge as imperative undertakings (Elbeltagi et al. 2022; Bytyqi and Agaj 2024), critical not only for the sustenance of societal needs but also for the preservation of environmental equilibrium (Raufu 2024).

Global temperature increases due to the accumulation of carbon dioxide (CO_2) and other greenhouse gases (GHGs) in the atmosphere, primarily caused by human activities (Stocker 2014; Bozhkov et al. 2022). Consequently, extreme weather events such as droughts and floods have become more frequent and destructive, posing severe impacts on communities, cities, and agricultural activities worldwide (Santos et al. 2024). North Africa is particularly vulnerable to these climate change impacts, with General Circulation Models (GCMs) from the fifth phase of the coupled model Intercomparison project (CMIP5) indicating a gradual rise in annual temperatures higher than the global average (IPCC 2013) Furthermore, the exacerbation of water deficits through increased evaporation worsens conditions (Shaiq et al. 2024; Aldughairi 2025), leading to salinization of coastal aquifers and reduced land areas suitable for agriculture (Radhouane 2013). The projected population growth in the Middle East and North Africa (MENA) region, estimated to reach around 700 million by 2050 (Roudi-Fahimi and Kent 2007), further intensifies the stress on water resources (Zerouali et al. 2023).

Indeed, evapotranspiration stands as a linchpin in the intricate web of the hydrological cycle, significantly affecting the delicate water balance of any given region. Within the context of Egypt, potential evapotranspiration (PET) assumes a paramount role, exerting a profound influence on water availability, agricultural productivity, and the broader dynamics of the ecosystem (Remini and Hallouche 2005; Elagib et al. 2024). The ability to comprehend and precisely forecast PET emerges as indispensable for the formulation and implementation of effective water resource management strategies throughout the country (El-kenawy et al. 2022). The Fourth Assessment Report of the Intergovernmental Panel on Climate Change (IPCC) also forecasts a significant temperature rise and decrease in total precipitation over the MENA region (Pachauri and Reisinger 2007). This trend is expected to further strain water resources, with PET demand escalating and exacerbating water stress in the region. PET plays a critical role in the global terrestrial hydrological cycle, influencing water needs for different crops, and serving as a key parameter in assessing hydrological impacts such as meteorological droughts, water balance analysis, and irrigation project design (Abdullah et al. 2015; Zerouali et al. 2024b).

The authors of (Feng et al. 2017) emphasized the importance of PET estimates at different temporal scales, with daily or sub-daily estimates crucial for determining plant water requirements and irrigation scheduling, while monthly and annual estimates aid in assessing long-term trends and climate feedback mechanisms. However, accurate PET estimation is challenging and relies on complex equations and methodologies. The Penman-Monteith (PM) method, considered a standard for PET calculation, requires various meteorological inputs and specific thresholds, posing limitations under extreme dry conditions (Brutsaert and Parlange 1998). In situations where meteorological variables necessary for PM calculations are unavailable, alternative methods such as

the Hargreaves–Samani (HS) (Hargreaves and Allen 2003) method offer a viable option due to their simplicity and reliance on temperature and precipitation data alone (Shahidian et al. 2012; Fisher and Pringle III 2013). The HS method has been widely employed in various studies globally, demonstrating good performance in semiarid and arid regions and providing reasonable accuracy in data-scarce areas (López-Urrea et al. 2006; Traore et al. 2010; Traore and Guven 2013). Moreover, the HS method is considered suitable for PET estimation under climate change scenarios (Li et al. 2018). Recent studies, such as those by (Anwar et al. 2021; Spinoni et al. 2021), highlight the importance of considering factors like vegetation cover changes, soil moisture, and temperature in PET simulations using regional climate models (RCMs). However, such corrections have not been conducted for Egypt's RCMs to date.

The HS method has been widely utilized in various studies, showcasing its versatility and effectiveness in PET estimation. For instance, the authors of (Khalil et al. 2015) utilized remote sensing products to estimate water loss from agricultural lands using the HS method, demonstrating its applicability in assessing agricultural water management practices. Similarly, (Cobaner et al. 2017) investigated the performance of the modified HS equation in PET estimation, highlighting its precision compared to Penman-Monteith (PM) observations. They emphasized the need to improve the HS method by incorporating actual lysimeter measurements to address uncertainties arising from empirically calculated parameters in the PM equation. Moreover, (Abdel Wahab et al. 2018) employed the regional climate model (RegCM4) to estimate water loss under the RCP4.5 scenario, underscoring the utility of RCMs in assessing climate change impacts on PET. The authors of Giménez and García-Galiano (2018) utilized an ensemble of regional climate models (RCMs) to analyze the influence of climate change on PET, demonstrating the capability of RCMs to capture variations in PET according to historical observations.

Additionally, Srivastava et al. (2018) applied the HS method and the Variable Infiltration Capacity (VIC-3L) land surface model to simulate actual evapotranspiration (ET) while respecting observed PM data. Their study highlighted the reasonable accuracy of standardized-HS and VIC-3L models in estimating regional and grid-scale variability of ET, particularly in data-scarce regions where field-scale measured data is limited. These studies collectively reinforce the robustness and versatility of the HS method in PET estimation across various climatic conditions and geographical scales. Till the present day, bias-correction methods have not been employed to reduce the PET uncertainty. To address the lack of correction for Regional Climate Models (RCMs) in Egypt for both historical and future periods, the following steps will be undertaken:

1. Spatial Analysis of Simulated PET: The spatial pattern of simulated PET will be examined for the historical period (1986–2005) and PET anomalies will be analyzed in time segments spanning from 2021–2100 under two future scenarios: Representative Concentration Pathway (RCP) 4.5 and RCP 8.5. This analysis will provide insights into the historical trends and future projections of PET across Egypt, allowing for a comprehensive understanding of the impacts of climate change on evapotranspiration patterns.

2. Bias Correction of Simulated PET: The simulated PET data will be bias-corrected with respect to the Climatic Research Unit (CRU) product for the period spanning from 1981–2005. This correction process will be conducted

for twelve specific locations across Egypt. By aligning the simulated PET data with observational-based datasets, any biases in the RCM outputs will be mitigated, ensuring the accuracy of PET estimates.

3. Projection Adjustment of PET: The projected PET data for the two future scenarios (RCP 4.5 and RCP 8.5) will be corrected using the Linear Regression Model (LRM) approach. This correction will be performed for the same twelve locations, utilizing data from both the RegCM4 model and CRU dataset from the historical period. By adjusting the projected PET data, discrepancies between RCM simulations and observational datasets will be addressed, resulting in more reliable future PET projections.

The methodology and experimental design for these steps will be detailed in Section 2 of the paper, providing comprehensive insights into the study area and the approach undertaken. Section 3 will present the results of the study, including spatial analysis findings, bias-corrected PET data, and adjusted projections. Finally, Section 4 will offer a discussion of the results and their implications for understanding the impacts of climate change on evapotranspiration patterns in Egypt, concluding with recommendations for future research and policy implications.

2. Materials and Methods

2.1. Study area

Egypt occupies the northeastern edge of the African continent, covering an expansive area of approximately one million km^2. It is bordered by the Mediterranean Sea to the north, the Gaza Strip, Palestine, and the Red Sea to the east, Sudan to the south, and the Libyan Arab Jamahiriya to the west. The country stretches approximately 1,080 km from north to south and around 1,100 km from east to west. Geographically, Egypt features a vast desert plateau punctuated by the Nile Valley and Delta; both collectively encompass about 4% of the nation's landmass. The landscape rises on both sides of the valley, reaching heights of approximately 1,000 m a.s.l. in the east and 800 m a.s.l. in the west. Mount Catherine in Sinai stands as Egypt's loftiest peak, towering at 2,629 m a.s.l., while the Qattara Depression in the northwest marks its lowest point, lying at 133 m b.s.l.

Climatically, Egypt experiences arid summers and mild winters. Also, it is characterized by sparse, erratic rainfall. Annual precipitation varies widely, with the northern coastal region receiving up to 200 mm annually, while the southern areas virtually receive none, averaging a mere 51 mm yearly. Summer temperatures soar to staggering levels, ranging from 38°C to 43°C, with southern and western desert regions witnessing extremes of up to 49°C. Conversely, the Mediterranean coastal zones boast cooler temperatures, peaking at around 32°C. Moreover, Egypt's agricultural calendar revolves around two distinct crop seasons: the summer season, spanning from April to September, and the winter season, covering October to March. Rice cultivation dominates the summer months, while winter sees the predominance of wheat harvesting (Hereher 2013).

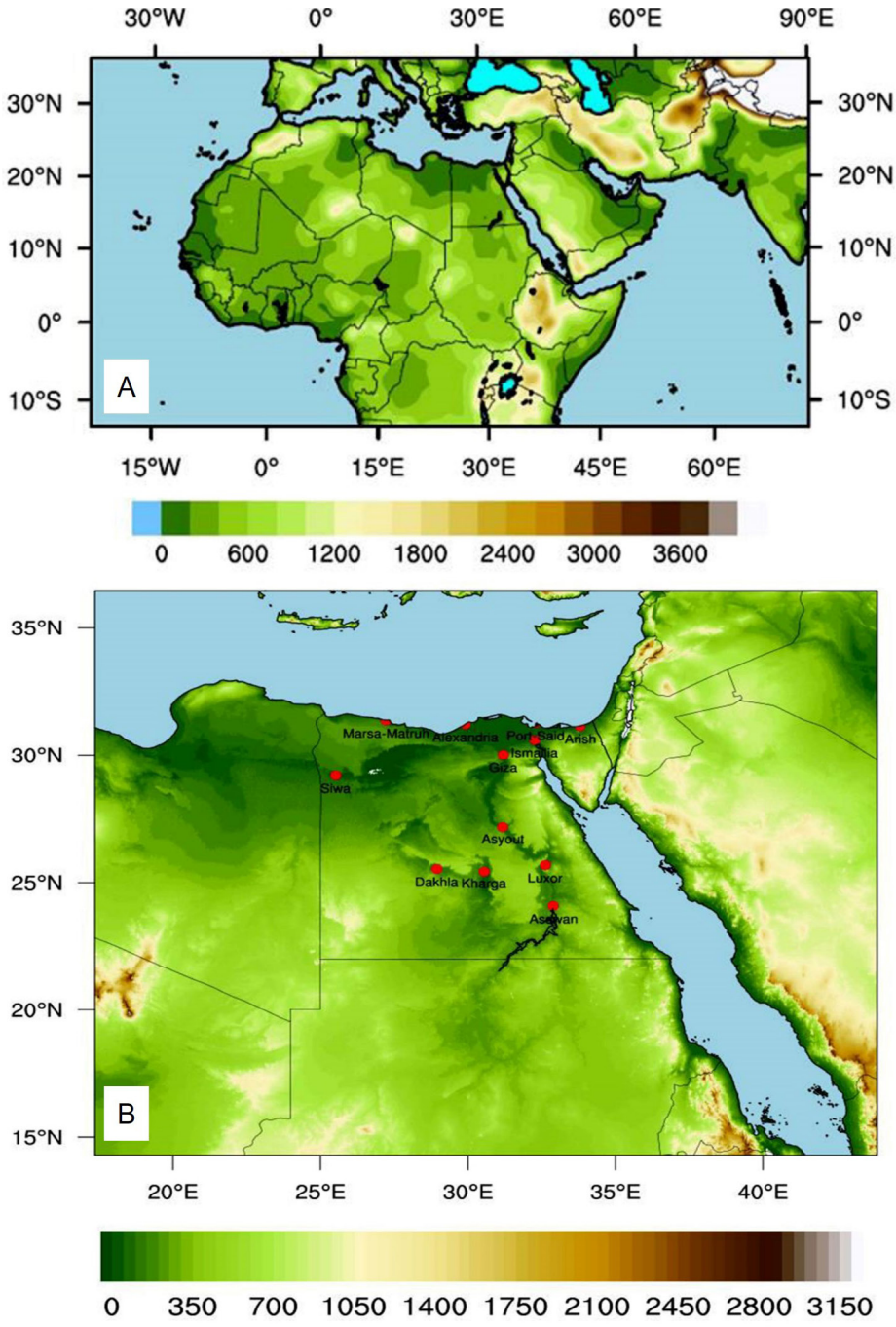

Figure 1. Representation of **A** the coarse domain and **B** nested domain (lower panel).

2.2. Potential evapotranspiration computing

The PET was calculated using various empirical equations commonly used in climate modeling. (Allen et al. 1994) provided one such equation, which involves pan evaporation (Ep) and a pan coefficient (Kp). Another equation by (Kjelgaard and Stockle 2001) incorporates factors such as surface net radiation (Rn), heat storage in soil (G), vapour pressure deficit (VPD), and aerodynamic and surface resistances to vapour transport (ra and rs). Additionally, the

Hargreaves-Samani (HS) (Hargreaves and Allen 2003) method was employed due to its suitability for calculating PET under climate change scenarios (Li et al. 2018). These equations consider meteorological variables such as 2-meter air temperature, relative humidity, wind speed, extraterrestrial radiation (Ra), and global incident solar radiation (Rs). In the present work, the PET was calculated as follow (Hargreaves and Allen 2003):

$$\mathrm{PET_{HS}} = 0.0135 \times \mathrm{R_S} \times (\mathrm{T_{mean}} + 17.8) \quad (1)$$

where R_s is the global incident solar radiation (expressed in mm day^{-1} to match the PET unit following Allen et al. 1998). T_{mean} is the daily mean air temperature and it is expressed in degree Celsius.

The relative PET changes were calculated following

$$\mathrm{PET_{relative\ changes}} = \frac{\mathrm{PET_{future\ annual}} - \mathrm{PET_{present\ annual}}}{\mathrm{PET_{present\ annual}}} \quad (2)$$

The PET anomaly was assessed spatially, focusing on the periods 2061–2080 and 2081–2100, and comparing the results under the RCP4.5 and RCP8.5 scenarios.

2.3. Model description and experiment design

This study employed the Abdus Salam International Centre for Theoretical Physics (ICTP) regional climate model version 4.7 (hereafter referred to as RegCM-4.7.0) (Giorgi et al. 2012). RegCM is a limited area model renowned for its capability in conducting long-term simulations within Intercomparison projects and process studies (Qian et al. 2010), as well as future climate projections (Giorgi et al. 2009). In this study, the third version of the Community Climate Model (CCM3) (Kiehl et al. 1996) was utilized for the radiation scheme, with the boundary layer scheme of (Holtslag and Boville 1993), the Grell convection scheme over land (Grell 1993), and the Emanuel convection scheme over the ocean (Emanuel 1991). This specific physical configuration was carefully selected after conducting numerous sensitivity studies using ERA-Interim reanalysis as a lateral boundary condition (EIN15) (Dee et al. 2011). A comprehensive description of the RegCM4 model can be found in (Giorgi et al. 2012). Recent applications of the RegCM4 model have extensively explored the potential impact of land-surface processes, including runoff, on simulating surface climate (Anwar et al. 2019; Wang et al. 2021), terrestrial carbon cycle (Anwar and Diallo 2021), and potential evapotranspiration (Anwar et al. 2021). This study encompasses two domains:

1. The coarse domain covers the MENA region with a horizontal grid spacing of 50 km, consisting of 235 grid points in the zonal direction and 121 grid points in the meridional direction. It is centred at latitude 19.5° and longitude 24.5°.

2. The nested domain covers Egypt and its surrounding regions with a horizontal grid spacing of 20 km, comprising 121 grid points in both the zonal and meridional directions. It is centred at latitude 25.5° and longitude 30.5°.

It is important to highlight that gradual downscaling (of that the MPI-ESM-MR) was employed through a coarse domain, and then to a nested domain (to provide high resolution meteorological information). Fig. 1 illustrates the

dimensions of the domains and the topography height for both the coarse and nested domains. The Earth System Model of the Max Planck Institute (MPI-ESM) of medium resolution (MR; 96 × 192 grid points, i.e., 1.875 × 1.875 horizontal degree resolution) was utilized to drive the RegCM4 model with the lateral boundary condition (LBC) and sea surface temperature (SST). The MPI-ESM, developed by Giorgetta et al. (2013), is an Earth System Model that integrates the atmosphere, ocean, and land surface, facilitating the exchange of energy, momentum, water, and carbon dioxide. The MPI-ESM integrates various components: the atmospheric component of ECHAM6 (Stevens et al. 2013), the ocean component of MPIOM (Jungclaus et al. 2013), the land component of JSBACH (Reick et al. 2013), and the ocean biogeochemistry component of HAMOCC (Ilyina et al. 2013). The OASIS3 program facilitates the coupling between the atmosphere, land, ocean, and biogeochemistry. Model simulations were conducted over two time periods: the historical period from 1981 to 2005 and the future period from 2006 to 2100, considering both the moderate future scenario RCP4.5 and the extreme future scenario RCP8.5.

It is noteworthy that while calculating the PET using the PM method is feasible with the 4.7 version of the RegCM, this specific calculation hasn't been tested. Therefore, the HG method was employed to compute the PET in this study, following the recommendation of (Cobaner et al. 2017; Abdel Wahab et al. 2018; Giménez and García-Galiano 2018; Srivastava et al. 2018). Additionally, the choice of the HG method is supported by Egypt's climatic characteristics outlined in study area section, which includes hot dry summers and mild winters, making the HG method a suitable option for PET computation in this context.

2.4. Observational data

In Egypt, the measurement of PET is crucial for various purposes such as monitoring agricultural activity, assessing water needs, and monitoring hydrological and drought conditions over different time intervals, including daily, seasonal, and annual periods. However, obtaining in-situ PET measurements using the PM method for an extended duration is not feasible. Therefore, in this study, the Climate Research Unit (CRU) dataset version 4.05 (Harris et al. 2020) was utilized as a reliable source of observational data. The CRU dataset is widely regarded as the best available reference for PET data and is commonly used as the ground truth for observational purposes in global PET assessments (Droogers and Allen 2002; Mitchell and Jones 2005; Sperna Weiland et al. 2012).

The CRU product encompasses a range of variables crucial for climate analysis, including cloud cover, diurnal temperature range, frost day frequency, PET, precipitation, 2-m mean temperature, maximum and minimum air temperature, and vapour pressure. These variables are monthly averaged and integrated over the extensive period from 1901 to 2020, providing a comprehensive dataset for climate research. The CRU product is available in a spatial resolution of 0.5 × 0.5 horizontal degrees, facilitating detailed analysis at regional and global scales. Notably, the CRU product has been employed in previous studies to enhance the accuracy of future rainfall projections in Egypt using the RegCM4 model (Elmenoufy et al. 2017). In our current study, we utilize the CRU gridded

product to refine PET estimates derived from the RegCM4 model output. This correction process is applied to both historical data and projections for two future scenarios (RCP4.5 and RCP8.5) across twelve specific locations, as outlined in Table 1.

3. Results

3.1. Spatial pattern of 2-m annual mean air temperature and PET under two future scenarios

In the previous section, it was emphasized that changes in PET can be monitored using the 2-m mean air temperature as a proxy (see eq. 2). Consequently, it is paramount to examine the future changes projected for the 2-m mean air temperature under the two future scenarios. This section initiates by discussing the spatial distribution of the simulated 2-m mean air temperature and PET during the reference period (1986–2005), subsequently addressing the alterations anticipated under the two future scenarios. Fig. 2 illustrates the projected changes in the 2-m mean air temperature (TMP) across Egypt for the period 2021–2100 under the RCP4.5 future scenario, segmented into four-time intervals: 2021–2040, 2041–2060, 2061–2080, and 2081–2100, compared to the reference period 1986–2005. This time frame aligns with the scope covered in the Arab Climate Change Assessment Report (ESCWA 2017). In the initial interval (2021–2040), the Western, Eastern Coast, and Delta regions display an increase in TMP ranging from 0.5 to 1°C, while Upper Egypt experiences a decrease in TMP by 0.5 to 1°C relative to the reference period (Fig. 2b). Moving to Fig. 2c, a rise in TMP is observed particularly in the Western desert (by 1 to 1.5°C), whereas Upper Egypt witnesses a slight decrease of 0.5°C during the 2041–2060 period. However, the scenario changes notably in the subsequent time segments (2061–2080 and 2081–2100), where an overall increase in TMP (ranging from 1 to 2°C) is observed across Egypt except for Upper Egypt (Fig. 2D–E).

Under the RCP8.5 future scenario, the 2-m TMP exhibits a similar increase to that observed in the time segments 2021–2040 and 2041–2060 (Fig. 3B–C). However, during the subsequent time segments 2061–2080 and 2081–2100, TMP demonstrates a more substantial increase, ranging from 3 to 5°C across Egypt, particularly noticeable in the time segment 2081–2100 (Fig. 3D–E). These findings suggest that both future scenarios align regarding the rate of TMP increase during the period 2021–2060, while the divergence between the two scenarios becomes apparent in the period 2061–2100, particularly during the time segment 2081–2100. As previously mentioned, changes in the 2-m TMP directly influence PET patterns. Therefore, the observed changes in TMP (Figs 2–3) are mirrored in the simulated future PET (Li et al. 2018). For example, under the RCP4.5 scenario, the simulated PET exhibits an increase (ranging from 0.1 to 0.3 mm day^{-1}) along the Western Coast and in the Western desert during the time segment 2021–2040 (Fig. 4B). This increase in PET corresponds to the TMP rise in these regions (Fig. 2B). Similarly, during the time segment 2041–2060, the RegCM4 model indicates an increase in simulated PET over Western Egypt, the Western Desert, and the Delta regions (Fig. 4C).

In the time segments 2061–2080 and 2081–2100, the RegCM4 model indicates an overall increase in simulated PET (ranging from 0.1 to 0.3 mm day^{-1} compared to the reference period) across Egypt, aligning with the observed increase in simulated TMP (Fig. 4D–E). Conversely, under the RCP8.5 scenario, the PET changes are less pronounced in the time segment 2021–2040, with fluctuations of around ±0.1 mm day^{-1} (Fig. 5B). However, from 2041 to 2060, the RegCM4 model projects an increase in simulated PET (by 0.1 to 0.3 mm day^{-1}) across Egypt (Fig. 5C), reflecting the observed changes in TMP. Notably, following the TMP patterns, the RegCM4 model predicts a higher increase in simulated PET (ranging from 0.3 to 0.6 mm day^{-1}) in the time segments 2061–2080 and 2081–2100 compared to the earlier periods (Fig. 5D). Finally, in the time segment 2081–2100, the RegCM4 model projects the most substantial increase in simulated PET across most of Egypt, with values ranging from 0.5 to 0.9 mm day^{-1} (Fig. 5E).

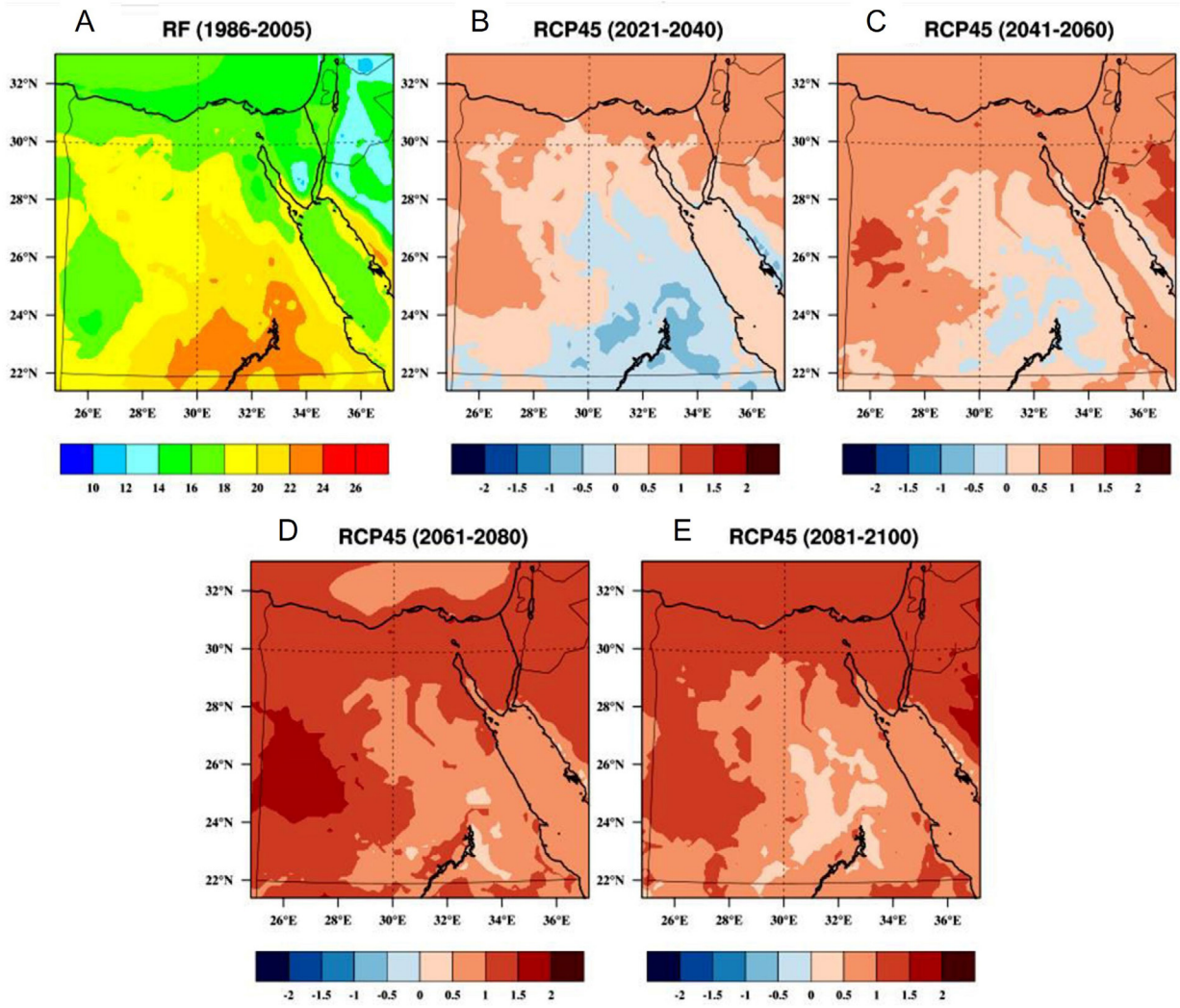

Figure 2. Annual average 2-m air temperature (hereafter TMP; in degrees Celsius) over Egypt during 1986–2005 (RF) **A** and the potential change during the period 2021–2040 **B** the period 2041–2060 **C** the period 2061–2080 **D** the period 2081–2100 **E** according to the RCP4.5 scenario.

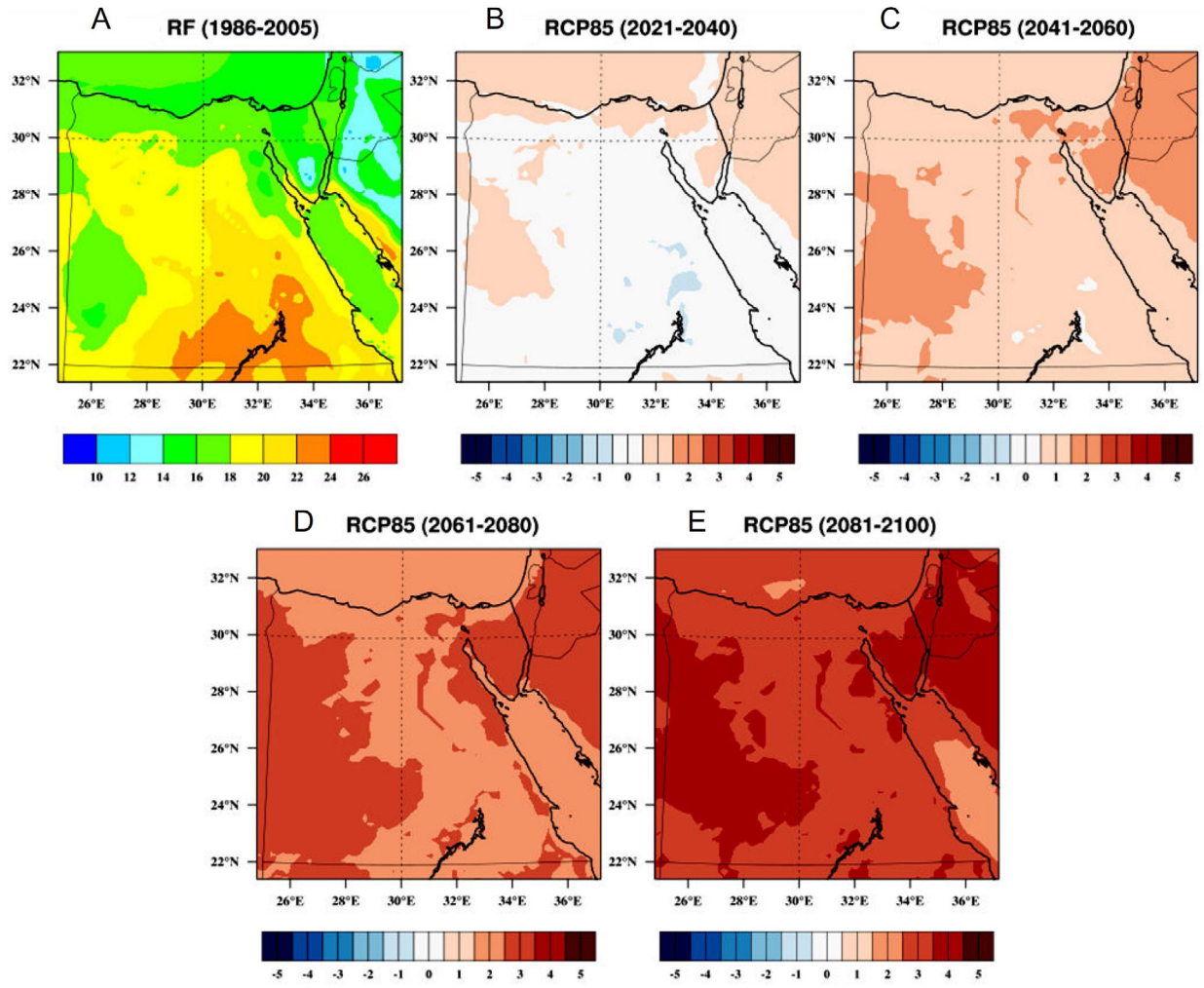

Figure 3. Annual average 2-m air temperature (in degrees Celsius) over Egypt during 1986–2005 (RF) **A** and the potential change during the period 2021–2040 **B** the period 2041–2060 **C** the period 2061–2080 **D** the period 2081–2100 **E** according to the RCP8.5 scenario.

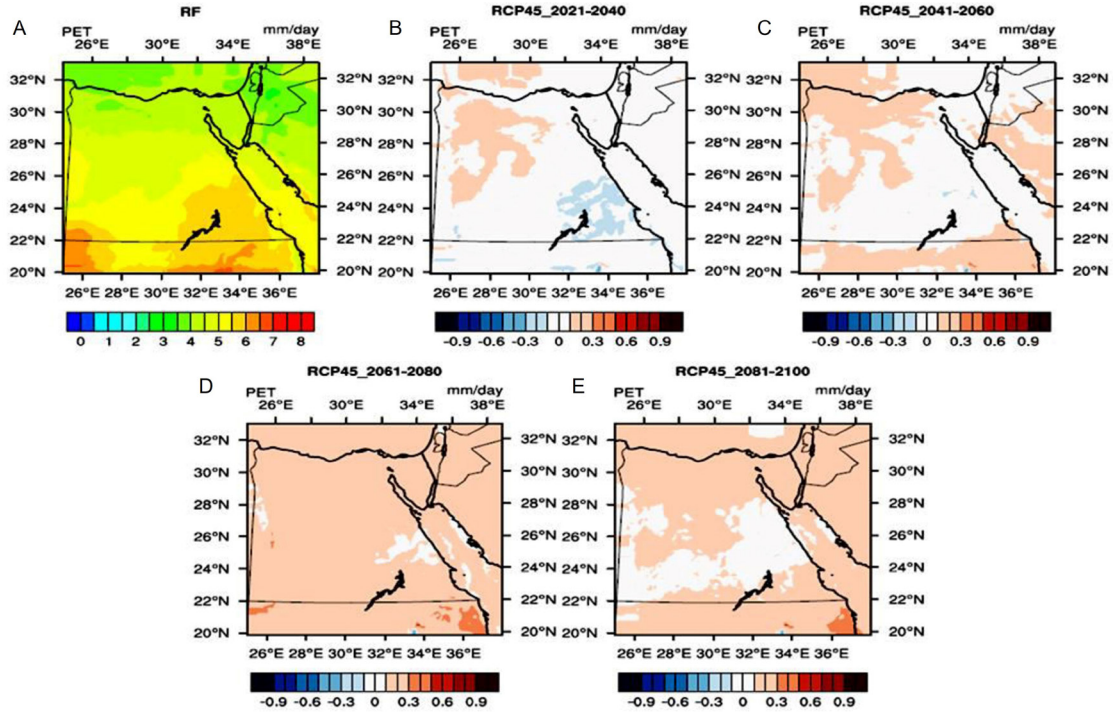

Figure 4. Representation of the average evapotranspiration (mm/day) over Egypt during 1986–2005 (RF) **A** and potential change during the period 2021–2040 **B** the period 2041–2060 **C** the period 2061–2080 **D** the period 2081–2100 **E** according to the RCP4.5 scenario.

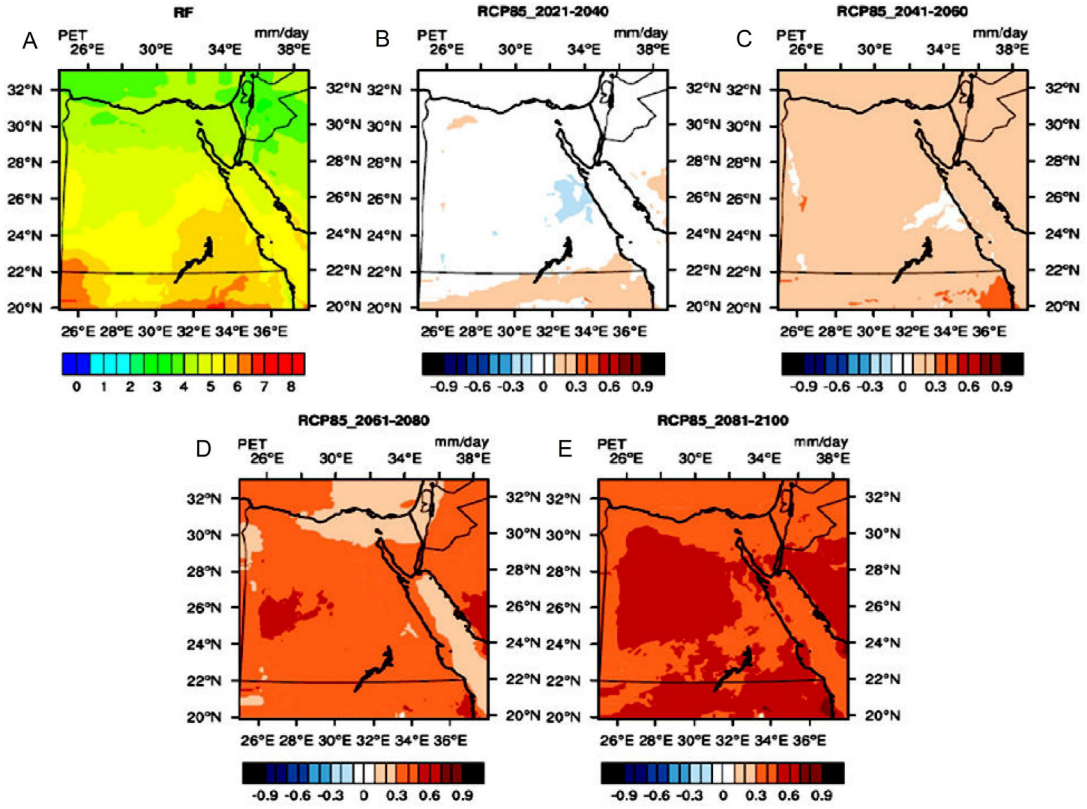

Figure 5. Representation of the average evapotranspiration (mm/day) over Egypt during 1986–2005 (RF) **A** and potential change during the period 2021–2040 **B** the period 2041–2060 **C** the period 2061–2080 **D** the period 2081–2100 **E** according to the RCP8.5 scenario.

3.2. Correcting the PET in the historical period and future scenarios

The performance of the RegCM4 model was evaluated with respect to the CRU gridded product for twelve locations, each representing different climate zones of Egypt (Table 1). These locations include Alexandria, Marsa Matruh, and Siwa for the northern zone; Ismailia, Port Said, and Arish for the eastern zone; Giza and Asyout for the Lower Egypt zone; Dakhla and Kharga for the Middle Egypt zone; and Luxor and Asswan for the Upper Egypt zone. To enhance the performance of the RegCM4 model, the LRM approach was employed by generating a scatter plot between the RegCM4 model output and the CRU observational-based product during the historical period from 1981 to 2005. The authors of (Shiri et al. 2012, 2014) demonstrated notable improvements in model performance when employing the LRM approach between model output and observed data. The LRM model was applied to the raw RegCM4 output to ensure accurate calculation of simulated PET compared to the CRU gridded product. Performance was assessed using statistical metrics such as mean bias (MB; calculated as CRU minus RegCM4) and standard deviation ratio (SD; the ratio between the standard deviation of the RegCM4 and the standard deviation of the CRU).

Fig. 6 displays the monthly time series of PET compared with CRU data for the historical period before and after applying the LRM method across the locations outlined in Table 1. Generally, the RegCM4 demonstrates good skill in capturing the monthly variability relative to the CRU dataset; however, it tends to underestimate or overestimate monthly PET depending on the specific location. Specifically, in Port Said, the RegCM4 significantly underestimates PET, particularly during the summer months (June–July–August), as compared to CRU data. Conversely, at Ismailia, the RegCM4 notably overestimates PET, while at Arish; it slightly underestimates PET compared to CRU data. The observed discrepancies at these locations can be attributed to uncertainties associated with the simulated 2-m mean air temperature and global incident solar radiation from the reanalysis product (not shown). However, significant improvement in the performance of the RegCM4 model was noted when the LRM approach was applied. Table 1 illustrates these improvements: before applying the LRM, Port Said had a mean bias (MB) of -0.34 mm day^{-1} and a standard deviation ratio (SD) of 1.25, which improved to -0.003 mm day^{-1} and 0.97, respectively, after applying the LRM. Similarly, Ismailia exhibited a MB of +1.15 mm day^{-1} and SD of 0.785 before the LRM, which improved to -0.02 mm day^{-1} and 0.99 with the LRM. Finally, for Arish, the MB was +0.5 mm day^{-1} with an SD of 0.94 before the LRM, which improved to +0.005 mm day^{-1} and 0.98 post-LRM application.

In Alexandria, the RegCM4 slightly underestimates PET compared to the CRU, with a mean bias (MB) of +0.73 mm day^{-1} and a standard deviation (SD) of 0.93 before the application of the LRM. However, after implementing the LRM, the RegCM4 exhibits superior performance, closely aligning with the CRU, resulting in an MB of -0.005 mm day^{-1} and an SD of 0.98. In Marsa Matruh, the RegCM4 shows a tendency to severely overestimate PET during summer months and slightly underestimate it during winter months (December–January–February) in comparison to the CRU. Quantitatively, this difference is evident as the mean bias (MB) is -0.27 mm day^{-1} and the SD is 1.58 before applying the LRM. After

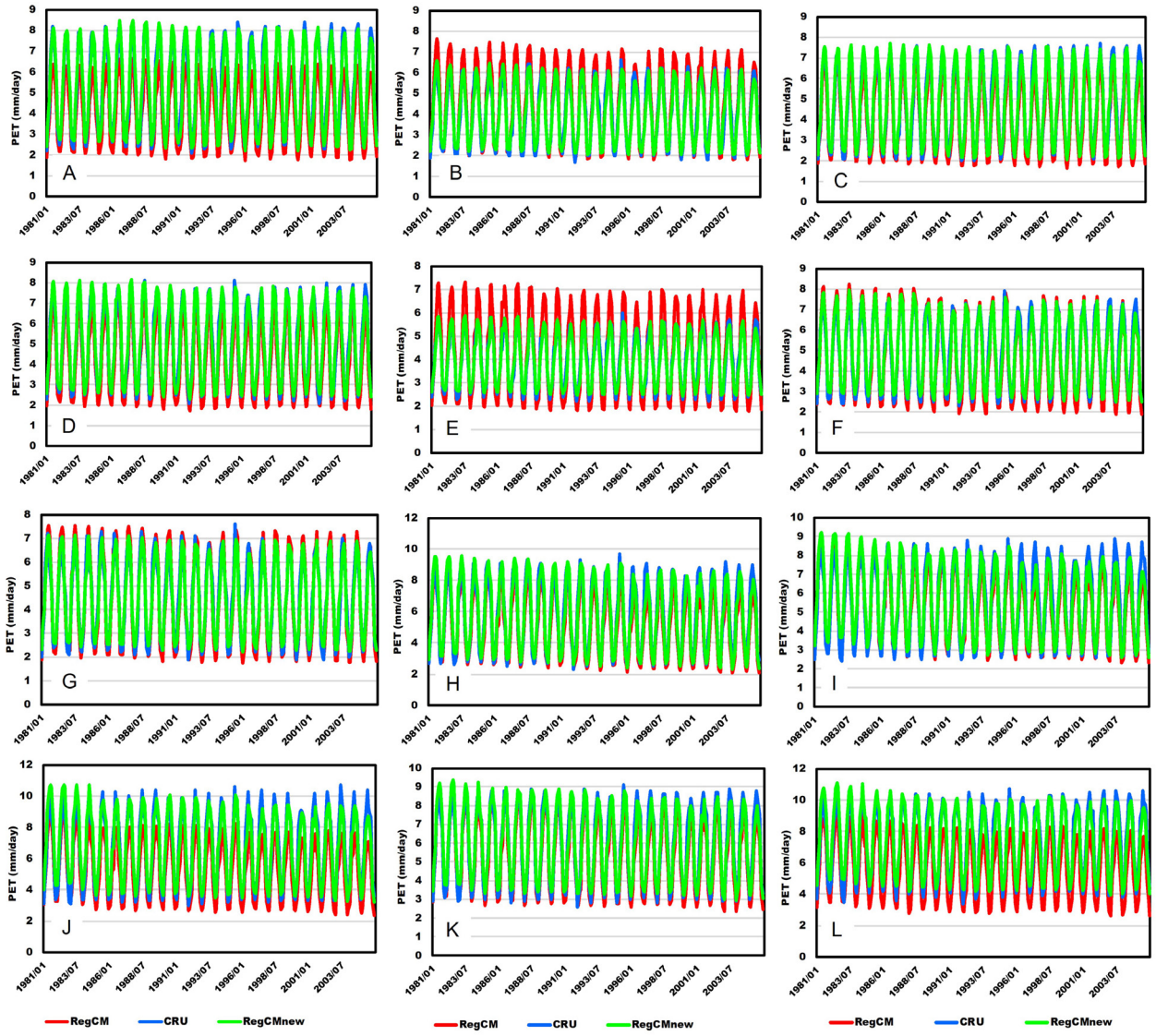

Figure 6. Representation of the monthly times series of Potential Evapotranspiration (PET; in mm/day) of by the RegCM4 in the historical period (1981–2005) of the twelve locations in comparison with the CRU product (in red), before applying the linear regression model (RegCM; in blue) and after applying the linear regression model (RegCMnew; in green) **A** Port Said **B** Ismailia **C** Arish **D** Alexandria **E** Marsa Matrush **F** Siwa **G** Giza **H** Asyout **I** Dakhla **J** Kharga **K** Luxor **L** Asswan.

implementing the LRM, the MB becomes nearly zero, indicating a much-improved alignment between the RegCM4 and CRU with a corresponding SD of 0.85. This suggests that the model slightly underestimates PET compared to the CRU and demonstrates the enhanced performance of the RegCM4 when the LRM is utilized. Similarly, in Siwa, the RegCM4 tends to overestimate PET during summer months relative to the CRU, as indicated by an MB of +0.21 mm day^{-1} and an SD of 1.13. However, with the application of the LRM, the RegCM4 exhibits superior performance in PET estimation, with an MB approaching zero mm day^{-1} and an SD of 0.97.

At Giza, the RegCM4 tends to overestimate PET, especially during the summer months (June, July, and August), when compared to the CRU. This overes-

timation may stem from the RegCM4's tendency to overestimate the 2-m mean air temperature in the reanalysis product. However, with the implementation of the LRM, the RegCM4 demonstrates improved capability in PET estimation, aligning more closely with the CRU. Quantitatively, the mean bias (MB) decreases from +0.07 mm day^{-1} to around zero mm day^{-1}, and the SD decreases from 1.13 to 0.96 after using the linear model. Conversely, at Asyout, the RegCM4 exhibits a declining trend in PET, resulting in close agreement with the CRU during the period 1981–1990. However, for the remaining period, the model severely underestimates PET, with an MB of +0.68 mm day^{-1} and an SD of 0.91. After implementing the LRM, the RegCM4 closely aligns with the CRU data during the period 1981–1990 and exhibits slight underestimation for the remaining period at Asyout, with a mean bias (MB) of -0.06 mm day^{-1} and a SD of 1.02. Similarly, at Dakhla and Kharga, the RegCM4 initially demonstrates a response similar to that observed at Asyout. However, there are notable differences in the values of MB and SD. Before applying the LRM, the MB ranges from 1.37 to 1.66, and the SD ranges from 0.82 to 0.87. Subsequently, after applying the LRM, the MB decreases significantly to near zero (around -0.002 mm day^{-1}), and the SD increases to 0.95–0.96.

At Luxor and Asswan, the RegCM4 initially underestimates PET relative to the CRU, with Asswan exhibiting a greater underestimation compared to Luxor. However, following the application of the LRM, the RegCM4 demonstrates improved accuracy in simulating PET, aligning closely with the CRU data. Before implementing the LRM, Luxor exhibits a mean bias (MB) of +0.52 mm day^{-1} and a SD of 0.99, while after LRM application, the MB becomes approximately zero mm/day and the SD decreases to 0.96. Given that PET calculations rely on eq. 1 (previous section), future changes in 2-m mean air temperature directly influence future PET levels. To project relative future PET changes for the twelve locations, the following steps are necessary:

1. Calculate the mean PET using the corrected RegCM4 output during the historical period.
2. Apply the LRM to correct the projected PET values for both RCP4.5 and RCP8.5 scenarios.
3. Calculate the relative PET changes according to the methodology outlined in (Nistor et al. 2019).

Fig. 7 illustrates the corrected relative future projections of PET for the twelve locations under the RCP4.5 and RCP8.5 scenarios. Notably, the relative changes in PET at Port Said remain within the range of -5% to +5% compared to the historical period from 2006 to 2042 under both scenarios. Subsequently, a slight increase of approximately 2% is projected under the RCP4.5 scenario, while a larger increase of around +12% is observed under the RCP8.5 scenario, consistent with earlier findings. Similarly, future changes in PET at Ismaila and Alexandria follow a comparable pattern to Port Said. However, at Arish, PET fluctuations range between -5% and +5% from 2006 to 2050, followed by significant increases reaching approximately +9% under RCP4.5 and up to 13% under RCP8.5 after 2050. Conversely, at Marsa Matruh, PET changes fluctuate between -3% and +3% from 2006 to 2045 under both scenarios, with subsequent increases reaching around +5% under RCP4.5 and approximately +8% under RCP8.5.

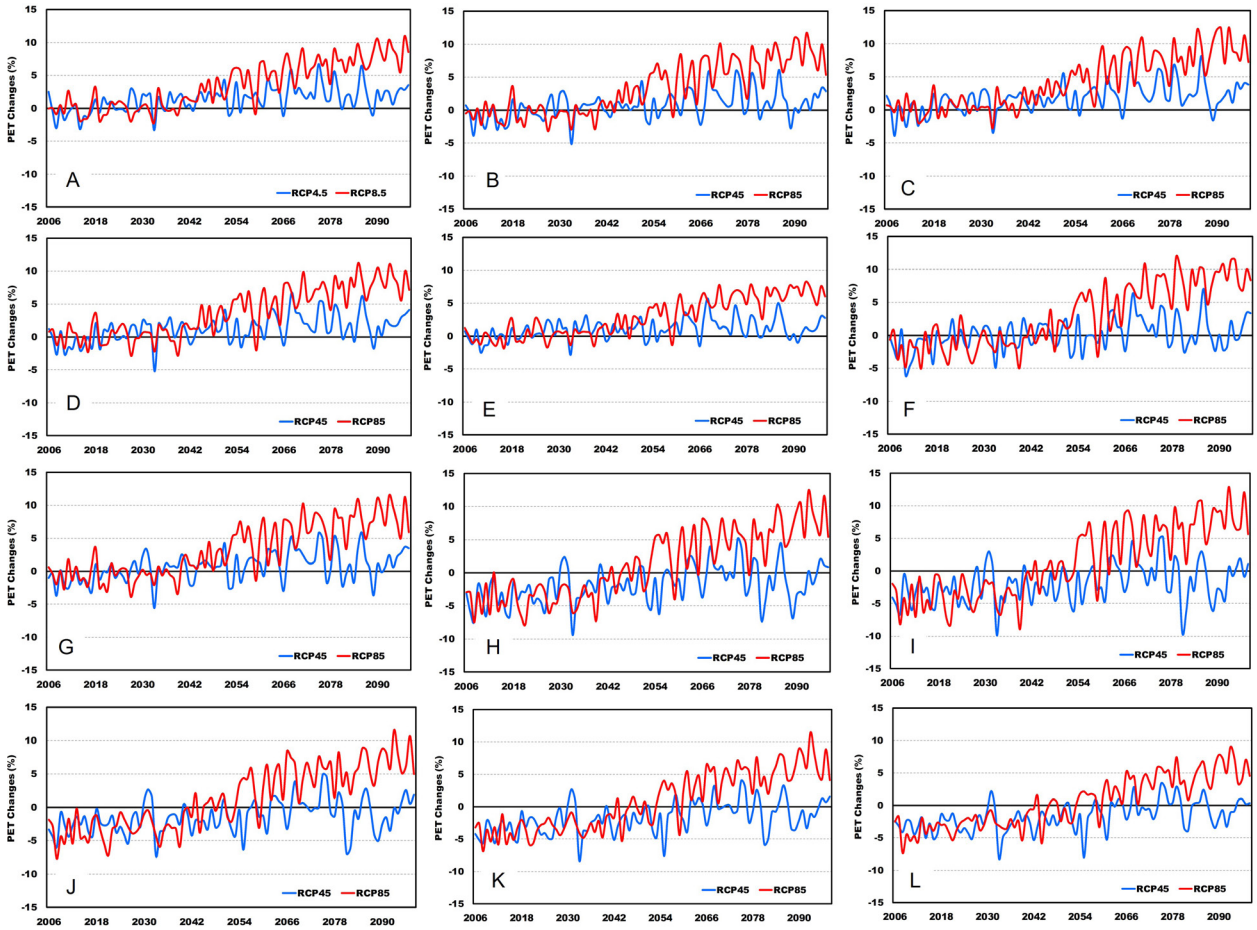

Figure 7. Representation of the shows the future corrected PET changes (in %) under the two future scenarios (RCP4.5; in blue) and (RCP8.5; in red) for the twelve locations **A** Port Said **B** Ismailia **C** Arish **D** Alexandria **E** Marsa Matrush **F** Siwa **G** Giza **H** Asyout **I** Dakhla **J** Kharga **K** Luxor **L** Asswan.

Despite the similarities in climate conditions between Marsa Matruh and Siwa, there are notable differences in the future projections of PET between these two locations. In Siwa, future PET changes fluctuate between -6% and +4% under both scenarios from 2006 to 2045, followed by continuous increases reaching approximately +7% under RCP4.5 and up to around +13% under RCP8.5 thereafter. Conversely, at Giza, future PET changes range between -6% and +5% from 2006 to 2045, with a slight increase of up to +6% under RCP4.5 and a gradual increase of up to +12% under RCP8.5. At Asyout, Dakhla, and Kharga, the future changes in projected PET exhibit the largest fluctuations under both scenarios, ranging from -10% to +5% from 2006 to 2045. Subsequently, under RCP4.5, the relative changes stabilize at +5%, while under RCP8.5, they gradually increase up to +12%. In Asswan, future PET changes fluctuate between -10% and +3% under RCP4.5 and between -7% and +5% under RCP8.5 from 2006 to 2045. Following this period, the future projected PET continues to increase steadily by 3% under RCP4.5 and gradually by up to +9% under RCP8.5.

Table 1. RegCM4 output correction at various locations.

Station	Lat	Long	RegCM4 output correction using LRM	Mean corrected PET in the historical period (in mm/day)	MB (in mm/day)		SD ratio (SDRegCM / SDCRU)	
					before	after	before	after
Port Said	31.28	32.23	PETcorr = 0.9641 × PETraw	5.25	1.15	-0.02	0.785	0.99
Alexandria	31.20	29.95	PETcorr = 1.057 × PETraw + 0.48	5.03	0.73	-0.005	0.93	0.98
Arish	31.08	33.83	PETcorr = 1.049 × PETraw + 0.294	4.74	0.5	0.00	0.94	0.98
Marsa Matruh	31.20	27.20	PETcorr = 0.617 × PETraw + 1.362	4.00	-0.27	0.00	1.58	0.85
Ismailia	30.60	32.26	PETcorr = 0.779 × PETraw + 0.635	4.08	-0.34	-0.003	1.25	0.97
Giza	30.05	31.22	PETcorr = 0.847 × PETraw + 0.748	4.52	0.07	0.00	1.13	0.96
Asyout	27.05	31.02	PETcorr = 1.12 × PETraw	5.81	0.68	-0.06	0.91	1.02
Luxor	25.66	32.70	PETcorr = 0.968 × PETraw + 0.696	5.99	0.52	0.00	0.99	0.96
Asswan	23.96	32.78	PETcorr = 1.097 × PETraw + 1.103	7.37	0.42	-0.005	0.9	0.94
Siwa	29.26	25.48	PETcorr = 0.861 × PETraw + 0.864	4.93	0.21	0.00	1.13	0.97
Dakhla	25.48	29.00	PETcorr = 1.049 × PETraw + 0.159	5.65	1.66	-0.002	0.87	0.96
Kharga	25.45	30.53	PETcorr = 1.16 × PETraw + 0.502	6.76	1.37	0.00	0.82	0.95

4. Discussion

In the Observational data section was emphasized that changes in PET can be monitored using the 2-m mean air temperature as a proxy (eq. 2). Consequently, it is paramount to examine the future changes projected for the 2-m mean air temperature under the two future scenarios. This section initiates by discussing the spatial distribution of the simulated 2-m mean air temperature and PET during the reference period (1986–2005), subsequently addressing the alterations anticipated under the two future scenarios. Fig. 2 illustrates the projected changes in the 2-m TMP across Egypt for the period 2021–2100 under the RCP4.5 future scenario, segmented into four-time intervals: 2021–2040, 2041–2060, 2061–2080, and 2081–2100, compared to the reference period 1986–2005. This time frame aligns with the scope covered in the Arab Climate Change Assessment Report (ESCWA 2017). In the initial interval (2021–2040), the Western, Eastern Coast, and Delta regions display an increase in TMP ranging from 0.5 to 1°C, while Upper Egypt experiences a decrease in TMP by 0.5 to 1°C relative to the reference period (Fig. 2B). Moving to Fig. 2C, a rise in TMP is observed particularly in the Western desert (by 1 to 1.5°C), whereas Upper Egypt witnesses a slight decrease of 0.5°C during the 2041–2060 period.

However, the scenario changes notably in the subsequent time segments (2061–2080 and 2081–2100), where an overall increase in TMP (ranging from 1 to 2°C) is observed across Egypt except for Upper Egypt (Fig. 2D–E). PET serves as a crucial variable in evaluating hydrological and agricultural activities, as well as monitoring regional droughts. The Food and Agriculture Organization (FAO) recommends the Penman-Monteith (PM) method for PET calculations. However, employing the PM method presents challenges due to specific thresholds and the requirement for an unlimited moisture supply (Brutsaert and Parlange 1998). Additionally, uncertainties in various meteorological inputs can amplify PET calculation errors, as the PM equation is nonlinear. Moreover, the application of the PM method in version 4.7 and beyond has not undergone comprehensive testing (Potential evapotranspiration computing section). To address these challenges, an empirical equation with minimal meteorological inputs is essential to track PET changes on daily or longer time scales, using a 2-meter TMP as a proxy. Consequently, the Horton-Smith (HS) method was chosen as an alternative option for calculating simulated PET from the RegCM4 output. In this study, the RegCM4 was downscaled by the MPI-ESM-MR over the MENA region and nested over the Egypt domain during the reference period 1980–2005, considering the two future scenarios: RCP4.5 and RCP8.5.

The model's performance was assessed against CRU data, revealing a gradual increase in projected PET from the North zone to the Upper Egypt zone, consistent with findings reported in previous studies (Attaher et al. 2006; Terink et al. 2013; Farag et al. 2016). Furthermore, PET experienced a moderate increase under the RCP4.5 scenario and a more substantial increase under the RCP8.5 scenario, particularly during the time segments 2061–2080 and 2081–2100. This underscores the necessity for adopting adaptation and mitigation strategies in the distant future to manage the rising temperatures and PET levels. Across the twelve locations detailed in Table 1, the RegCM4 model demonstrated the ability to replicate monthly variability based on CRU observational data. However, it exhibited variations in PET estimates depending on the location, with improved performance observed when employing the LRM Notably, the most significant fluctuations in future projected PET changes were observed at Asyout, Dakhla, Kharga, and Luxor, particularly under the RCP8.5 scenario. It's important to mention that this study offers an initial insight into projecting PET in Egypt using a single high-resolution regional climate model, with PET bias corrected for both historical and future scenarios using the LRM approach. The present study relied on downscaling one GCM from the pool of the Fifth phase of the Coupled Model Intercomparison Project (CMIP5) (Taylor et al. 2012). Future research will address key aspects:

1. Utilizing multi-GCMs (CMIP5/CMIP6) (Taylor et al. 2012; Eyring et al. 2016) and their ensembles to further examine the impact of climate change on mean temperature (T_{mean}), solar radiation (R_s), and PET.
2. Investigating the potential influence of aerosols on simulated mean temperature (T_{mean}), solar radiation (R_s), and, subsequently, PET.
3. Evaluating the performance of RegCM4 with high-resolution gridded PET products e.g., (Singer et al. 2020; Singer et al. 2021) alongside CRU data to account for uncertainties in observational-based datasets.
4. Apply direct downscaling to reduce the uncertainty of the calculated T_{mean} and eventually PET following Anwar et al. (2023).

5. Adopting the physical parameterization and the calibrated version of the HS equation following (Anwar and Olusegun 2024).
6. Initializing the RegCM4 regional climate model with the Century reanalysis soil moisture product following (Anwar 2024).

5. Conclusion

This study utilized a high-resolution regional climate model (RegCM4) to compute the PET for Egypt, employing a simple empirical method (Hargreaves-Samani; HS) instead of the more complex Penman-Monteith method. The choice of the HS method is particularly advantageous as it requires fewer meteorological variables, many of which are derived empirically, simplifying the calculations involved. The application of the LRM demonstrated significant value in reducing uncertainty in PET estimates, both for the historical reference period and under various future scenarios.

The results indicate that while the RegCM4 model effectively captures the monthly variability of PET, discrepancies remain among different locations, particularly under varying climatic conditions. The LRM improved the alignment of model outputs with observational data from the CRU, highlighting its effectiveness in enhancing model performance. However, several limitations must be acknowledged. The reliance on a single regional climate model restricts the generalizability of the findings, as different models can yield varying results based on their underlying assumptions and parameterizations. Additionally, the availability and quality of historical meteorological data can affect the accuracy of PET calculations, with limited access to comprehensive datasets potentially introducing biases in the model outputs. The HS method, while straightforward, may not fully capture the complexities of evapotranspiration processes, particularly in regions characterized by high variability in microclimates. Furthermore, projections under the RCP4.5 and RCP8.5 scenarios are contingent on the accuracy of climate models and their assumptions about greenhouse gas emissions, which can change over time.

To enhance the robustness and reliability of PET estimations in Egypt, future research should incorporate multiple regional climate models and Global Climate Models (GCMs) to compare outputs and reduce uncertainty in PET estimates. Utilizing ensemble approaches can provide a more comprehensive understanding of potential climate impacts. Additionally, integrating high-resolution gridded PET products could improve accuracy and account for spatial variability that a single model may overlook. Expanding the range of meteorological inputs used in empirical methods will also refine accuracy, as variables such as humidity and wind speed play significant roles in PET dynamics. Investigating localized climate effects will yield insights into region-specific trends and anomalies, facilitating more tailored adaptation strategies. Finally, establishing long-term monitoring stations for climate variables across diverse regions in Egypt will help gather high-quality data, enabling more accurate modeling and forecasting of PET under changing climatic conditions. By addressing these limitations and implementing the recommended strategies, future research can significantly advance our understanding of potential evapotranspiration dynamics in Egypt, ultimately informing effective water resource management and agricultural practices in the face of climate change.

Acknowledgements

The authors would like to express gratitude to Kyoto University of Advanced Science International and Start-up Grants in this study.

References

Abda Z, Zerouali B, Chettih M, Guimarães Santos CA, De Farias CAS, Elbeltagi A (2022) Assessing machine learning models for streamflow estimation: a case study in Oued Sebaou watershed (Northern Algeria). Hydrological Sciences Journal 67: 1328–1341. https://doi.org/10.1080/02626667.2022.2083511

Abdel Wahab MM, Essa YH, Khalil AA, Elfadli K, Panegrossi G (2018) Water Loss in Egypt Based on the Lake Nasser Evaporation andAgricultural Evapotranspiration. EnvironmentAsia 11: 192204. https://doi.org/10.14456/EA.2018.33

Abdullah SS, Malek MA, Abdullah NS, Kisi O, Yap KS (2015) Extreme Learning Machines: A new approach for prediction of reference evapotranspiration. Journal of Hydrology 527: 184–195. https://doi.org/10.1016/j.jhydrol.2015.04.073

Aldughairi A (2025) Climate change assessment in middle and northern Saudi Arabia: Alarming trends. DYSONA - Applied Science 6: 60–69. https://doi.org/10.30493/das.2024.477412

Allen RG, Smith M, Perrier A, Pereira LS (1994) An update for the definition of reference evapotranspiration. ICID Bulletin 43(2): 1–34.

Anwar SA (2024) On the Sensitivity of the Potential Evapotranspiration of Egypt to Different Initial Conditions of the Soil Moisture Using a High-resolution Regional Climate Model. Journal of Biomedical Research & Environmental Sciences 5: 501–514. https://doi.org/10.37871/jbres1920

Anwar SA, Diallo I (2021) A RCM investigation of the influence of vegetation status and runoff scheme on the summer gross primary production of Tropical Africa. Theoretical and Applied Climatology 145: 1407–1420. https://doi.org/10.1007/s00704-021-03667-0

Anwar SA, Mamadou O, Diallo I, Sylla MB (2021) On the Influence of Vegetation Cover Changes and Vegetation-Runoff Systems on the Simulated Summer Potential Evapotranspiration of Tropical Africa Using RegCM4. Earth Systems and Environment 5: 883–897. https://doi.org/10.1007/s41748-021-00252-3

Anwar SA, Olusegun CF (2024) Simulating the Potential Evapotranspiration of Egypt Using the RegCM4: Sensitivity to the Land Surface and Boundary Layer Parameterizations. Hydrology 11: 121. https://doi.org/10.3390/hydrology11080121

Anwar SA, Srivastava A, Zerouali B (2023) On the role of land-surface hydrology schemes in simulating the daily maximum and minimum air temperatures of Australia using a regional climate model (RegCM4). Journal of Water and Climate Change 14: 989–1011. https://doi.org/10.2166/wcc.2023.512

Anwar SA, Zakey AS, Robaa SM, Abdel Wahab MM (2019) The influence of two land-surface hydrology schemes on the regional climate of Africa using the RegCM4 model. Theoretical and Applied Climatology 136: 1535–1548. https://doi.org/10.1007/s00704-018-2556-8

Attaher S, Medany MA, Abdel Aziz AA, El-Gindy A (2006) Irrigation-water demands under current and future climate conditions in Egypt. Misr Journal of Agricultural Engineering 23(4): 1077–1089.

Bozhkov P, Grigorov B, Sarafov A (2022) Comparative analysis of soil organic carbon in selected river catchments. Journal of the Bulgarian Geographical Society 47: 45-51. https://doi.org/10.3897/jbgs.e98660

Brutsaert W, Parlange MB (1998) Hydrologic cycle explains the evaporation paradox. Nature 396: 30–30. https://doi.org/10.1038/23845

Bytyqi V, Agaj T (2024) Spatio-temporal distribution of renewable freshwater resources and their availability in Kosovo—an analysis from the Eastern Region. Journal of the Bulgarian Geographical Society 50: 35-52. https://doi.org/10.3897/jbgs.e115814

Cobaner M, Citakoğlu H, Haktanir T, Kisi O (2017) Modifying Hargreaves–Samani equation with meteorological variables for estimation of reference evapotranspiration in Turkey. Hydrology Research 48: 480–497. https://doi.org/10.2166/nh.2016.217

Dee DP, Uppala SM, Simmons AJ, Berrisford P, Poli P, Kobayashi S, Andrae U, Balmaseda MA, Balsamo G, Bauer P, Bechtold P, Beljaars ACM, Van De Berg L, Bidlot J, Bormann N, Delsol C, Dragani R, Fuentes M, Geer AJ, Haimberger L, Healy SB, Hersbach H, Hólm EV, Isaksen L, Kållberg P, Köhler M, Matricardi M, McNally AP, Monge-Sanz BM, Morcrette J -J., Park B -K., Peubey C, De Rosnay P, Tavolato C, Thépaut J -N., Vitart F (2011) The ERA-Interim reanalysis: configuration and performance of the data assimilation system. Quarterly Journal of the Royal Meteorological Society 137: 553–597. https://doi.org/10.1002/qj.828

Droogers P, Allen RG (2002) Estimating reference evapotranspiration under inaccurate data conditions. Irrigation and Drainage Systems 16: 33–45. https://doi.org/10.1023/A:1015508322413

ESCWA (United Nations Economic and Social Commission for Western Asia) et al. (2017) Arab Climate Change Assessment Report – Main Report. Beirut, E/ESCWA/SDPD/2017/RICCAR/Report.

El-kenawy E-SM, Zerouali B, Bailek N, Bouchouich K, Hassan MA, Almorox J, Kuriqi A, Eid M, Ibrahim A (2022) Improved weighted ensemble learning for predicting the daily reference evapotranspiration under the semi-arid climate conditions. Environmental Science and Pollution Research 29: 81279–81299. https://doi.org/10.1007/s11356-022-21410-8

Elagib NA, Ali MMA, Schneider K (2024) Evaluation and bias correction of CRU TS4.05 potential evapotranspiration across vast environments with limited data. Atmospheric Research 299: 107194. https://doi.org/10.1016/j.atmosres.2023.107194

Elbeltagi A, Seifi A, Ehteram M, Zerouali B, Vishwakarma DK, Pandey K (2023) GLUE analysis of meteorological-based crop coefficient predictions to derive the explicit equation. Neural Computing and Applications 35: 14799–14824. https://doi.org/10.1007/s00521-023-08466-4

Elbeltagi A, Zerouali B, Bailek N, Bouchouicha K, Pande C, Santos CAG, Towfiqul Islam ARMd, Al-Ansari N, El-kenawy E-SM (2022) Optimizing hyperparameters of deep hybrid learning for rainfall prediction: a case study of a Mediterranean basin. Arabian Journal of Geosciences 15: 933. https://doi.org/10.1007/s12517-022-10098-2

Elmenoufy HM, Morsy M, Eid MM, El Ganzoury A, El-Hussainy FM, Wahab MMA (2017) Towards enhancing rainfall projection using bias correction method: case study Egypt. IJSRSET 3(6): 187–194.

Emanuel KA (1991) A scheme for representing cumulus convection in large-scale models. Journal of the Atmospheric Sciences 48(21): 2313–2329. https://doi.org/10.1175/1520-0469(1991)048%3C2313:ASFRCC%3E2.0.CO;2

Eyring V, Bony S, Meehl GA, Senior CA, Stevens B, Stouffer RJ, Taylor KE (2016) Overview of the Coupled Model Intercomparison Project Phase 6 (CMIP6) experimental de-

sign and organization. Geoscientific Model Development 9: 1937–1958. https://doi.org/10.5194/gmd-9-1937-2016

Farag AA, Abdrabbo AAM, el Sharkawi HM, Abou-Hadid AF (2016) Comparison between SERES and RCP scenarios in temperature and evapotranspiration under different climate zone. Journal of Environmental Science, Toxicology and Food Technology 10(11): 54–64.

Feng Y, Jia Y, Cui N, Zhao L, Li C, Gong D (2017) Calibration of Hargreaves model for reference evapotranspiration estimation in Sichuan basin of southwest China. Agricultural Water Management 181: 1–9. https://doi.org/10.1016/j.agwat.2016.11.010

Fisher DK, Pringle III HC (2013) Evaluation of alternative methods for estimating reference evapotranspiration. Agricultural Sciences 04: 51–60. https://doi.org/10.4236/as.2013.48A008

Giménez PO, García-Galiano SG (2018) Assessing Regional Climate Models (RCMs) Ensemble-Driven Reference Evapotranspiration over Spain. Water 10: 1181. https://doi.org/10.3390/w10091181

Giorgetta MA, Jungclaus J, Reick CH, Legutke S, Bader J, Böttinger M, Brovkin V, Crueger T, Esch M, Fieg K, Glushak K, Gayler V, Haak H, Hollweg H, Ilyina T, Kinne S, Kornblueh L, Matei D, Mauritsen T, Mikolajewicz U, Mueller W, Notz D, Pithan F, Raddatz T, Rast S, Redler R, Roeckner E, Schmidt H, Schnur R, Segschneider J, Six KD, Stockhause M, Timmreck C, Wegner J, Widmann H, Wieners K, Claussen M, Marotzke J, Stevens B (2013) Climate and carbon cycle changes from 1850 to 2100 in MPI-ESM simulations for the Coupled Model Intercomparison Project phase 5. Journal of Advances in Modeling Earth Systems 5: 572–597. https://doi.org/10.1002/jame.20038

Giorgi F, Coppola E, Solmon F, Mariotti L, Sylla M, Bi X, Elguindi N, Diro G, Nair V, Giuliani G, Turuncoglu U, Cozzini S, Güttler I, O'Brien T, Tawfik A, Shalaby A, Zakey A, Steiner A, Stordal F, Sloan L, Brankovic C (2012) RegCM4: model description and preliminary tests over multiple CORDEX domains. Climate Research 52: 7–29. https://doi.org/10.3354/cr01018

Giorgi F, Jones C, Asrar GR (2009) Addressing climate information needs at the regional level: the CORDEX framework. World Meteorological Organization (WMO) Bulletin 58(3): 175.

Grell GA (1993) Prognostic evaluation of assumptions used by cumulus parameterizations. Monthly Weather Review 121(3): 764–787. https://doi.org/10.1175/1520-0493(1993)121%3C0764:PEOAUB%3E2.0.CO;2

Hargreaves GH, Allen RG (2003) History and Evaluation of Hargreaves Evapotranspiration Equation. Journal of Irrigation and Drainage Engineering 129: 53–63. https://doi.org/10.1061/(ASCE)0733-9437(2003)129:1(53)

Harris I, Osborn TJ, Jones P, Lister D (2020) Version 4 of the CRU TS monthly high-resolution gridded multivariate climate dataset. Scientific Data 7: 109. https://doi.org/10.1038/s41597-020-0453-3

Hereher ME (2013) The status of Egypt's agricultural lands using MODIS Aqua data. The Egyptian Journal of Remote Sensing and Space Science 16: 83–89. https://doi.org/10.1016/j.ejrs.2013.03.001

Holtslag AAM, Boville BA (1993) Local versus nonlocal boundary-layer diffusion in a global climate model. Journal of Climate 6(10): 1825–1842. https://doi.org/10.1175/1520-0442(1993)006%3C1825:LVNBLD%3E2.0.CO;2

Ilyina T, Six KD, Segschneider J, Maier-Reimer E, Li H, Núñez-Riboni I (2013) Global ocean biogeochemistry model HAMOCC: Model architecture and performance as component of the MPI-Earth system model in different CMIP5 experimental reali-

zations. Journal of Advances in Modeling Earth Systems 5: 287–315. https://doi.org/10.1029/2012MS000178

IPCC (2013) Summary for Policymakers. In: Stocker T et al. (Ed.) Climate Change 2013: The Physical Science Basis. Contribution of Working Group I to the Fifth Assessment Report of the Intergovernmental Panel on Climate Change. Cambridge University Press, New York.

Jungclaus JH, Fischer N, Haak H, Lohmann K, Marotzke J, Matei D, Mikolajewicz U, Notz D, Von Storch JS (2013) Characteristics of the ocean simulations in the Max Planck Institute Ocean Model (MPIOM) the ocean component of the MPI-Earth system model. Journal of Advances in Modeling Earth Systems 5: 422–446. https://doi.org/10.1002/jame.20023

Khalil AA, Essa YH, Abdel-Wahab MM (2015) Evapotranspiration mapping over Egypt using MODIS/Terra satellite data. International Journal of Advanced Research 15(12): 512–522.

Kiehl J, Hack J, Bonan G, Boville B, Briegleb B, Williamson D, Rasch P (1996) Description of the NCAR Community Climate Model (CCM3). UCAR/NCAR, 7652 KBpp. https://doi.org/10.5065/D6FF3Q99

Kjelgaard JF, Stockle CO (2001) Evaluating surface resistance for estimating corn and potato evapotranspiration with the Penman–Monteith model. Transactions of the ASAE 44. https://doi.org/10.13031/2013.6243

Lasheen EA (2022) Against the Grain: A History and Policy Analysis of Rice, Water and the Edible Landscape in Egypt. PhD Thesis, Massachusetts Institute of Technology, Massachusetts, United States.

Li Z, Yang Y, Kan G, Hong Y (2018) Study on the Applicability of the Hargreaves Potential Evapotranspiration Estimation Method in CREST Distributed Hydrological Model (Version 3.0) Applications. Water 10: 1882. https://doi.org/10.3390/w10121882

López-Urrea R, Martín De Santa Olalla F, Fabeiro C, Moratalla A (2006) Testing evapotranspiration equations using lysimeter observations in a semiarid climate. Agricultural Water Management 85: 15–26. https://doi.org/10.1016/j.agwat.2006.03.014

Mitchell TD, Jones PD (2005) An improved method of constructing a database of monthly climate observations and associated high-resolution grids. International Journal of Climatology 25: 693–712. https://doi.org/10.1002/joc.1181

Nistor M, Mîndrescu M, Petrea D, Nicula A, Rai PK, Benzaghta MA, Dezsi Ş, Hognogi G, Porumb-Ghiurco CG (2019) Climate change impact on crop evapotranspiration in Turkey during the 21st Century. Meteorological Applications 26: 442–453. https://doi.org/10.1002/met.1774

Pachauri RK, Reisinger A (2007) Climate change 2007: Synthesis report. Contribution of working groups I, II and III to the fourth assessment report of the Intergovernmental Panel on Climate Change. IPCC.

Qian J-H, Robertson AW, Moron V (2010) Interactions among ENSO, the Monsoon, and Diurnal Cycle in Rainfall Variability over Java, Indonesia. Journal of the Atmospheric Sciences 67: 3509–3524. https://doi.org/10.1175/2010JAS3348.1

Radhouane L (2013) Climate change impacts on North African countries and on some Tunisian economic sectors. Journal of Agriculture and Environment for International Development (JAEID) 107(1): 101–113. https://doi.org/10.12895/jaeid.20131.123

Raufu IO (2024) Exploring the relationship between remote sensing-based vegetation indices and land surface temperature through quantitative analysis. Journal of the Bulgarian Geographical Society 50: 95-112. https://doi.org/10.3897/jbgs.e124098

Reick CH, Raddatz T, Brovkin V, Gayler V (2013) Representation of natural and anthropogenic land cover change in MPI-ESM. Journal of Advances in Modeling Earth Systems 5: 459–482. https://doi.org/10.1002/jame.20022

Remini B, Hallouche W. 2005. L'alluvionnement des retenues. Blida, Algérie: Edition Imprimerie Madani, 102 pp.

Roudi-Fahimi F, Kent MM (2007) Challenges and Opportunities—The Population of the Middle East and North Africa. Population Bulletin 62(2). Population Reference Bureau, Washington, DC.

Santos CAG, Do Nascimento GR, Freitas LMT, Batista LV, Zerouali B, Mishra M, Silva RMD (2024) Coastal evolution and future projections in Conde County, Brazil: A multi-decadal assessment via remote sensing and sea-level rise scenarios. Science of The Total Environment 915: 169829. https://doi.org/10.1016/j.scitotenv.2023.169829

Shahidian S, Serralheiro R, Serrano J, Teixeira J, Haie N, Santos F (2012) Hargreaves and Other Reduced-Set Methods for Calculating Evapotranspiration. In: Irmak A (Ed.), Evapotranspiration - Remote Sensing and Modeling. InTech. https://doi.org/10.5772/18059

Shaiq MA, Aiuby H, Hayat M (2024) Navigating drought in Kunduz province Afghanistan: insights from experts' perspectives. DYSONA - Applied Science. https://doi.org/10.30493/das.2024.442563

Shiri J, Kişi Ö, Landeras G, López JJ, Nazemi AH, Stuyt LCPM (2012) Daily reference evapotranspiration modeling by using genetic programming approach in the Basque Country (Northern Spain). Journal of Hydrology 414–415: 302–316. https://doi.org/10.1016/j.jhydrol.2011.11.004

Shiri J, Nazemi AH, Sadraddini AA, Landeras G, Kisi O, Fakheri Fard A, Marti P (2014) Comparison of heuristic and empirical approaches for estimating reference evapotranspiration from limited inputs in Iran. Computers and Electronics in Agriculture 108: 230–241. https://doi.org/10.1016/j.compag.2014.08.007

Singer MB, Asfaw DT, Rosolem R, Cuthbert MO, Miralles DG, MacLeod D, Quichimbo EA, Michaelides K (2021) Hourly potential evapotranspiration at 0.1° resolution for the global land surface from 1981-present. Scientific Data 8: 224. https://doi.org/10.1038/s41597-021-01003-9

Singer M, Asfaw D, Rosolem R, Cuthbert MO, Miralles DG, Miguitama EQ, MacLeod D, Michaelides K (2020) Hourly potential evapotranspiration (hPET) at 0.1degs grid resolution for the global land surface from 1981-present. https://doi.org/10.5523/BRIS.QB8UJAZZDA0S2AYKKV0OQ0CTP

Sperna Weiland FC, Tisseuil C, Dürr HH, Vrac M, Van Beek LPH (2012) Selecting the optimal method to calculate daily global reference potential evaporation from CFSR reanalysis data for application in a hydrological model study. Hydrology and Earth System Sciences 16: 983–1000. https://doi.org/10.5194/hess-16-983-2012

Spinoni J, Barbosa P, Bucchignani E, Cassano J, Cavazos T, Cescatti A, Christensen JH, Christensen OB, Coppola E, Evans JP, Forzieri G, Geyer B, Giorgi F, Jacob D, Katzfey J, Koenigk T, Laprise R, Lennard CJ, Kurnaz ML, Li D, Llopart M, McCormick N, Naumann G, Nikulin G, Ozturk T, Panitz H, Da Rocha RP, Solman SA, Syktus J, Tangang F, Teichmann C, Vautard R, Vogt JV, Winger K, Zittis G, Dosio A (2021) Global exposure of population and land-use to meteorological droughts under different warming levels and SSPs : A CORDEX -based study. International Journal of Climatology 41: 6825–6853. https://doi.org/10.1002/joc.7302

Srivastava A, Sahoo B, Raghuwanshi NS, Chatterjee C (2018) Modelling the dynamics of evapotranspiration using Variable Infiltration Capacity model and regionally calibrat-

ed Hargreaves approach. Irrigation Science 36: 289–300. https://doi.org/10.1007/s00271-018-0583-y

Stevens B, Giorgetta M, Esch M, Mauritsen T, Crueger T, Rast S, Salzmann M, Schmidt H, Bader J, Block K, Brokopf R, Fast I, Kinne S, Kornblueh L, Lohmann U, Pincus R, Reichler T, Roeckner E (2013) Atmospheric component of the MPI-M Earth System Model: ECHAM6. Journal of Advances in Modeling Earth Systems 5: 146–172. https://doi.org/10.1002/jame.20015

Stocker T (Ed.) (2014) Climate change 2013: the Physical Science Basis: Working Group I contribution to the Fifth Assessment Report of the Intergovernmental Panel on Climate Change. Cambridge University Press, New York, 1535 pp.

Taylor KE, Stouffer RJ, Meehl GA (2012) An Overview of CMIP5 and the Experiment Design. Bulletin of the American Meteorological Society 93: 485–498. https://doi.org/10.1175/BAMS-D-11-00094.1

Terink W, Immerzeel WW, Droogers P (2013) Climate change projections of precipitation and reference evapotranspiration for the Middle East and Northern Africa until 2050. International Journal of Climatology 33: 3055–3072. https://doi.org/10.1002/joc.3650

Traore S, Guven A (2013) New algebraic formulations of evapotranspiration extracted from gene-expression programming in the tropical seasonally dry regions of West Africa. Irrigation Science 31: 1–10. https://doi.org/10.1007/s00271-011-0288-y

Traore S, Wang Y-M, Kerh T (2010) Artificial neural network for modeling reference evapotranspiration complex process in Sudano-Sahelian zone. Agricultural Water Management 97: 707–714. https://doi.org/10.1016/j.agwat.2010.01.002

Wang X, Chen D, Pang G, Anwar SA, Ou T, Yang M (2021) Effects of cumulus parameterization and land-surface hydrology schemes on Tibetan Plateau climate simulation during the wet season: insights from the RegCM4 model. Climate Dynamics 57: 1853–1879. https://doi.org/10.1007/s00382-021-05781-1

Zerouali B, Bailek N, Islam ARMT, Katipoğlu OM, Ayek AAE, Santos CAG, Rajput J, Wong YJ, Abda Z, Chettih M, Elbeltagi A (2024a) Enhancing groundwater potential zone mapping with a hybrid analytical method: The case of semiarid basin. Groundwater for Sustainable Development 26: 101261. https://doi.org/10.1016/j.gsd.2024.101261

Zerouali B, Bailek N, Bouchouich K, Mawloud G, Kuriqi A, Sami Khafaga D, H. Alharbi A, M. El-kenawy E-S (2024b) Enhancing water security through advanced modeling: integrating deep learning and a novel metaheuristic optimization algorithm for accurate pan evaporation prediction. AQUA — Water Infrastructure, Ecosystems and Society: jws2024128. https://doi.org/10.2166/aqua.2024.128

Zerouali B, Chettih M, Abda Z, Mesbah M (2023) Future Hydroclimatic Variability Projections Using Combined Statistical Downscaling Approach and Rainfall-Runoff Model: Case of Sebaou River Basin (Northern Algeria). In: Pande CB, Moharir KN, Singh SK, Pham QB, Elbeltagi A (Eds), Climate Change Impacts on Natural Resources, Ecosystems and Agricultural Systems. Springer Climate. Springer International Publishing, Cham, 297–326. https://doi.org/10.1007/978-3-031-19059-9_11

Additional information

Conflict of interest

No conflict of interest was declared.

Ethical statement

No ethical statement was reported.

Funding

No funding was reported.

Author contributions

Conceptualization: SAA, BZ, LZ. Formal analysis: SAA, BZ, LZ. Writing - original draft: BZ, LZ, SAA. Writing - review and editing: YJW.

Author ORCIDs

Samy A Amwar https://orcid.org/0000-0002-4077-8648
Latifa Zhouri https://orcid.org/0000-0001-8401-6082
Bilel Zerouali https://orcid.org/0000-0003-4735-9750
Yong Jie Wong https://orcid.org/0000-0002-5254-5243

Data availability

All of the data that support the findings of this study are available in the main text or Supplementary Information. MPI-ESM-MR and EIN15 can be retrieved from http://www.clima-dods.ictp.it/RegCM4.